Journal of Applied Fluid Mechanics, Vol. 17, No. 8, pp. 1677-1686, 2024.
Available online at www.jafmonline.net, ISSN 1735-3572, EISSN 1735-3645.
https://doi.org/10.47176/jafm.17.8.2434

Study of the Thermal Buoyancy on the Smoke Flow in Tunnel Fires under the Coupled Effects of the Longitudinal Air-flow and the Tunnel Slope

B. Kalech†, M. Bouterra, and A. ElCafsi

LETTM, Faculty of Sciences of Tunis, El Manar University, 2092 Tunis, Tunisia

†Corresponding Author Email: ibrahim.kalech@fst.utm.tn

ABSTRACT

To understand the stratification of the smoke layer in a road tunnel, numerical simulations are employed to model tunnel fires with varying heat release rates. The different simulations cases are carried out with FDS (Fire dynamic simulations). These simulations are conducted to examine the influence of tunnel slope and longitudinal airflow on the smoke stratification along the downstream side of tunnel. The aim is to explore the relationship between longitudinal airflow and temperature ratio taking into account the tunnel slope. As a result, a quantitative analysis, based on Newman's theory, is conducted to assess the clarity of the smoke layer stratification, a Froude number (Fr = 0.63) is obtained. The slopes in tunnels can have a substantial impact on smoke flow during a fire, primarily driven by thermal buoyancy and the stack effect. With a slope less than 1.5°, the stratification improves. Similarly, clear stratification occurs when the longitudinal airflow is less than 1 m/s. However, a balance between inertia force and buoyancy force is crucial for maintaining clear stratification. Increasing both the longitudinal airflow and the tunnel slope serves to disturb the stratification of the smoke layer.

Article History

Received November 26, 2023
Revised February 24, 2024
Accepted February 25, 2024
Available online May 29, 2024

Keywords:

Smoke stratification
Froude Number
Longitudinal air-flow
Sloping tunnel

1. INTRODUCTION

Urban road tunnels are an effective means of alleviating traffic congestion for users. However, in the event of a tunnel fire, hot gases can travel along the tunnel ceiling, transporting dangerous and potentially lethal combustion byproducts over long distances. One significant factor contributing to this risk is the presence of soot within the smoke layer formed in the tunnel, which poses a threat to the safety of tunnel users.

Nevertheless, it is crucial to gain a clear understanding of the thermal properties of smoke in tunnel fires and the associated temperature distribution. These factors hold significant importance in the research on fire-induced smoke within tunnels, given the multitude of parameters upon which they rely. The study of temperature distribution and smoke layer stratification is conducted across various fire scenarios within tunnels, as documented in many references (Kalech et al., 2013; Ji et al., 2018; Zeng et al., 2018; Haddad et al., 2020; Kalech et al., 2020; Savalanpour et al., 2021).

Literature also includes studies on smoke movement within inclined tunnels. Researchers have systematically examined the impact of tunnel slopes on back-layering length, critical velocity, and temperature distribution during tunnel fires (Atkinson & Wu, 1996; Gwon Hyun et al., 2010; Hu et al., 2013; Yi et al., 2014; Weng et al., 2016; Wan et al. 2019; Han et al., 2020; Ko et al., 2010). These investigations hold substantial value as references for the design of longitudinal ventilation systems in inclined tunnels, contributing to improved safety and efficiency in such environments.

Chow et al. (2016) conducted a study on smoke movement utilizing natural ventilation in a sloped tunnel model. They examined the angles ranging from 3 to 9 degrees and discussed the presence of asymmetrical smoke temperature and velocity distribution both upstream and downstream of the fire location. This research provided insights into how tunnel slope and natural ventilation can affect smoke behavior in tunnel fires.

The maximum gas temperature beneath the ceiling in a tunnel fire is influenced by many factors. These factors

NOMENCLATURE

C_s	Smagorinsky constant (LES)	T_f	floor temperature
P_{rt}	turbulent Prandtl number	T_c	ceiling temperature
S_{ct}	turbulent Schmidt number	T_{avg}	average Temperature
g	acceleration of gravity	ΔT_{cf}	temperature difference between the ceiling temperature and floor temperature
C_p	specific heat	ΔT_{avg}	temperature difference between the average temperature and ambient temperature
ρ	density	H	tunnel height
Q	heat release rate of the fire	W	tunnel width
V_{avg}	average longitudinal velocity	L	tunnel length
U	velocity of longitudinal air-flow	h	shaft height
β	tunnel slope	w	shaft width
D^*	characteristic fire diameter	l	shaft length
Fr	Froude number	$\Delta x, \Delta y, \Delta z$	dimensions of the smallest grid cell

encompass the heat release rate of the fire source, the tunnel's geometry, and notably, the longitudinal velocity of air-flow.

Li et al. (2011) conducted experimental tests aimed at predicting a model of maximum temperature distribution below the tunnel ceiling, with a specific consideration for the longitudinal velocity. The correlation is hypothetically fitted as:

$$\Delta T_{max} = \begin{cases} \frac{Q^*}{u\, r^{1/3} H_d^{5/3}} & , u' > 0.19 \\ 17{,}5 \frac{Q^{*\,2/3}}{H_d^{5/3}} & , u' \leq 0.19 \end{cases} \quad (1);$$

Where $u' = \frac{u}{u^*}$ and $u^* = \left(\frac{Q_c g}{r \rho_a C_p T_a}\right)^{1/3}$

With ρ_a (kg/m^3) is the ambient air density, T_a ($°C$) is the ambient air temperature, H_d (m) is the height from the fire source to the tunnel ceiling, u (m/s) is the longitudinal velocity of air flow in the tunnel, r (m) is the radius of the fire source and Q_c (kw) is the convective heat release rate of fire source.

An experimental study was conducted by Hu et al. (2013) to investigate the impact of tunnel slope on the gas temperature beneath the ceiling. They modified the model originally proposed by Li et al. (2011) for predicting the maximum temperature, incorporating considerations for the tunnel's inclination.

Generally, the thermal stratification is a crucial aspect of the fire environment in confined spaces, such as tunnels. The balance between the thermal buoyancy force and the inertial force is a fundamental factor that governs the behavior of smoke stratification in tunnel fires. Understanding this balance is essential for effectively analyzing and managing fire safety in tunnel scenarios.

Yang et al. (2010) investigated the characteristics of fire-induced buoyant flow stratification, considering the impact of the mechanical exhaust rate at the ceiling. The observed stratification pattern was found to exhibit three distinct regimes. The relation between buoyancy force and inertia force was correlated using the Froude number and the Richardson number. The thermal stratification was influenced by forced air flow, operating through two distinct aspects.

Guo et al. (2021) investigated the distribution of smoke temperatures and smoke stratification under conditions of longitudinal ventilation, using the Newman's theory. Following their study, they developed prediction models for both smoke stable-stratification-length and the critical stratification velocity. These models are valuable tools for assessing and understanding smoke behavior and safety considerations in tunnel with longitudinal ventilation.

Newman (1984) developed a model that expresses the state of smoke stratification through the vertical temperature distribution. This model provides insights into how the temperature varies with height and can be used to understand the stratification state within the smoke layer. The correspondence by Newman can be expressed by Eq. (2):

$$\begin{cases} \frac{\Delta T_{cf}}{\Delta T_h} = 0.67 \left(\frac{\Delta T_{cf}}{\Delta T_{avg}}\right)^{0{,}77} & ; \frac{\Delta T_{cf}}{\Delta T_{avg}} \leq 1.7 \\ \frac{\Delta T_{cf}}{\Delta T_h} = 1 & ; \frac{\Delta T_{cf}}{\Delta T_{avg}} > 1.7 \end{cases} ; \quad (2)$$

Where ΔT_{cf} ($°C$); the temperature difference between the ceiling and floor, ΔT_h ($°C$); the temperature difference between the ceiling and the ambient temperature and ΔT_{avg} ($°C$) the temperature difference between the vertical average temperature and the ambient temperature.

When $\frac{\Delta T_{cf}}{\Delta T_{avg}} > 1.7$, $\frac{\Delta T_{cf}}{\Delta T_h} \approx 1$, the temperature at the floor almost is equal to ambient temperature, and the smoke layer is well stratified. When $\frac{\Delta T_{cf}}{\Delta T_{avg}} < 1.7$, $\frac{\Delta T_{cf}}{\Delta T_h} < 1$, the temperature is increased at the floor, the stratification of the smoke layer decreases at until it disappears. Finally, Newman (1984) proposed the correlation between the temperature ratio and the Froude number (Fr):

$$\frac{\Delta T_{cf}}{\Delta T_{avg}} = 1.5\, Fr^{-1} ; \quad (3)$$

Such as; $Fr = \frac{V_{avg}}{\sqrt{g\,H(\frac{\Delta T_{cf}}{\Delta T_{avg}})}}$, $V_{avg} = V\,\frac{T_{avg}}{T_a}$ (4)

Where $H(m)$ is the height of tunnel and $V(m/s)$ is the longitudinal velocity. Newman (1984) found that the Froude number equal to 0.9 ($\frac{\Delta T_{cf}}{\Delta T_{avg}} = 1.7$) is the criterion to distinguish the clear stratification of the smoke layer. Region I, with $\frac{\Delta T_{cf}}{\Delta T_{avg}} > 1.7$ or Fr < 0.9, represent the clear stratification of the smoke layer. Region II represent the less clear stratification region. Region III, with $\frac{\Delta T_{cf}}{\Delta T_{avg}} \leq 0.1$ or Fr ≥ 10, the smoke layer is no stratification.

Nyman and Ingason (2012) studied the smoke stratification with a reduced scale model tests and full scale tests. The correlation proposed is as follows:

$$\frac{\Delta T_{cf}}{\Delta T_{avg}} = 0{,}62\ Fr^{-1{,}58} \quad (5)$$

Nyman and Ingason (2012) determined a Froude number of 0.55 as a criterion for distinguishing clear stratification of the smoke layer in their research. This finding highlights the variability in the Froude number threshold across different studies and reinforces the importance of considering specific conditions and factors when assessing the smoke layer stratification. Furthermore, we mention that the effect of tunnel slope on temperature distribution and smoke flow stratification has not been adequately addressed in existing models.

By conducting this research, we aim to contribute to a better understanding of smoke stratification in inclined tunnels.

The lack study on the smoke flow stratification, with the longitudinal air flow in inclined tunnel, motivates a investigation in the current paper.

Hence, this paper intends to investigate the effect of tunnel slope on the smoke layer stratification with longitudinal airflow, and proposes a correlation between the stratification parameters.

2. NUMERICAL MODEL

An open source CFD software (FDS) is used in this study. FDS is a freely software available for public and has been widely used in fire modeling. FDS has undergone extensive validation and improvement efforts since its initial release in 2000. The model has been subjected to numerous validation exercises, calibrations, and studies focusing on temperature and velocity fields in fire scenarios. A detailed description of the model, along with validation examples, can be found in our reference (McGrattan et al., 2017a). However, for the purposes of this study, we utilized version 6.5 of Fire Dynamic Simulation (FDS).

FDS numerically solves the equations of the Navier-Stokes that is suitable for low-velocity, thermally-driven flows, with a primary focus on simulating the transport of smoke and heat originating from fires. The fundamental algorithm at its core is an explicit predictor-corrector scheme, which exhibits second-order accuracy in both spatial and temporal domains. The turbulence is addressed using the Smagorinsky model of Large Eddy Simulation (LES).

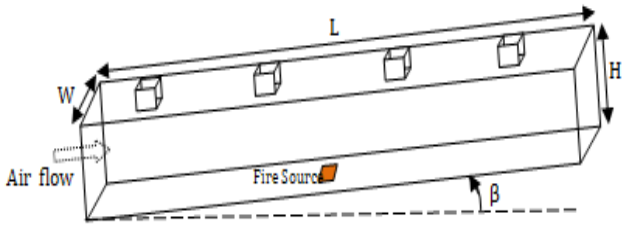

Fig. 1. Geometrical configuration

The constant of Smagorinsky, C_s, has been optimized over a range from 0.1 to 0.25 for various flow fields. For the tunnel fire, the Smagorinsky constant equal to 0.2 has been considered most appropriate, and for Pr_t and Sc_t are assumed to be constant they have equal to 0.2 and 0.5, respectively (Ji et al., 2013; McGrattan et al., 2017b, c; Kalech et al., 2020).

Furthermore, a combustion model based on the mixture fraction concept is used in FDS for large-eddy simulation. The fraction of the fuel converted to CO, y_{CO}, is related to the fraction of the efficiency of the soot, y_s. y_s value was set at 0.1 according to the "CRUDE OIL" (Hu et al. 2007; Kalech et al., 2020). The combustion model is integrated with a radiation model, which calculates thermal radiation transfer by solving the radiation transport equation for a gray gas.

2.1 Fire Scenario Analysis

In the current research, the tunnel model as shown in Fig. 1 is defined with the following dimensions: a length (L) of 300 m, a width (W) of 10 m, and a height (H) of 5.01 m. This tunnel features four openings or shafts. The first shaft is positioned 59 m from the left end of the tunnel. These four shafts are evenly distributed along the length of the tunnel, with a spacing of 58 m between each of them. Each shaft has a height of 0.334 m and a square area with dimensions of 2 m by 2 m for width (w) and length (l) of the shafts.

The tunnel model is made of “CONCRETE”. The physical properties of this material (thermal conductivity, density and specific heat) are specified in the FDS. The values used for the calculation are a thermal conductivity of 1,65 W/m K, density of 2500 kg/m^3 and specific heat of 0.88 kJ/kg K. The tunnel surfaces (walls, ceiling and floor) are thermally thick and smooth. At the wall surface, the default velocity condition provided by FDS was used (McGrattan et al., 2017b, c).

The fire source was positioned at the center of the tunnel, and three different heat release rates (HRR) were used: 4 MW, 10 MW, and 20 MW, which correspond to burning a car, bus, and light truck, respectively. To simulate the fire, a square heat source was employed with a cross-sectional area of 2 m by 2 m for an HRR of 10 MW. For the HRRs of 4 MW and 20 MW, the corresponding areas used were 2 m^2 and 6 m^2,

Table 1 Summary of all cases.

Heat release rate Q (MW)	Tunnel slope β (°)	Longitudinal air-flow U (m/s)
4	0, 3, 6	0, 1, 2, 3
10	0, 1.5, 3, 6	0, 0.5, 1, 2, 3
20	0, 3, 6	0, 1, 2, 3

respectively, as referenced in study of Kalech et al. (2020).

An inlet velocity boundary condition was set at the left end of the tunnel. The top of the four shafts and the right side of the tunnel are open to be naturally, without initial velocity. The ambient temperature and the ambient pressure were set as 20 °C and 101 kPa respectively in the series of simulations.

The tunnel can have different positions depending on the β, such as the angle defines the slope of the tunnel. However, each of these positions of tunnel will be subjected to different longitudinal velocities of air flow (0, 1, 2, 3 m / s) with the three powers (4MW, 10MW and 20MW). In this study, the slope values at 0° to 6°. The simulation cases are shown in the Table 1.

2.2 Sensitivity Study on the Grid System

In FDS, the grid size is an important parameter to be considered. The criterion $\left(\frac{D^*}{\Delta x}\right)$ is used for assessing the grid resolution (McGrattan et al., 2017b). It is better to assess the quality of the mesh in terms of this non-dimensional parameter, rather than an absolute mesh cell size (Ji et al., 2013; Kalech et al., 2020). Where D^* is a characteristic of fire diameter and Δx is the grid size;

$$D^* = \left(\frac{Q}{\rho_a C_p T_a \sqrt{g}}\right)^{\frac{2}{5}} . \quad (6)$$

The authors Ji et al. (2013), McGrattan et al., 2017b, Fan et al. (2018) and Kalech et al. (2020) have proved that a mesh size of about 10% of the characteristic diameter is acceptable to guarantee a reliable results, $\Delta x = 0.1D^*$. In this study, the smallest fire size is 4MW.The corresponding value of $0.1D^*$ is about 0.167 m.

A non-uniform mesh distribution was utilized to maintain an adequate level of accuracy in the solution. The entire tunnel domain was divided into three continuous sub-domains. The region near the fire source, spanning from x =140 m to x =160 m, was designated as the Middle Domain. The upstream area, covering x = 0 m to x =140 m, is defined as the Left Domain. The downstream region, covering x = 160 m to x = 300 m, is defined as the Right Domain.

Typically, the value of Δx ranged from $0.0625D^*$ to $0.25D^*$, as referenced in many studies (Ji et al., 2013; Fan et al., 2018; Huang et al., 2018).

Following the grid independence test, the grid system was established with $\Delta x = 0.1D^*$ for the Middle Domain and Δx=0.2 D* for the Left and Right Domains, as noted in study of Huang et al. (2018).

For this study, the grid system was set with Δx = 0.125m for the Middle Domain and Δx = 0.25m for the Left and Right Domains, with Δy=0.2m and Δz=0.167m, as indicated in many studies (Ji et al., 2013; Fan et al., 2018; Huang et al. 2018).

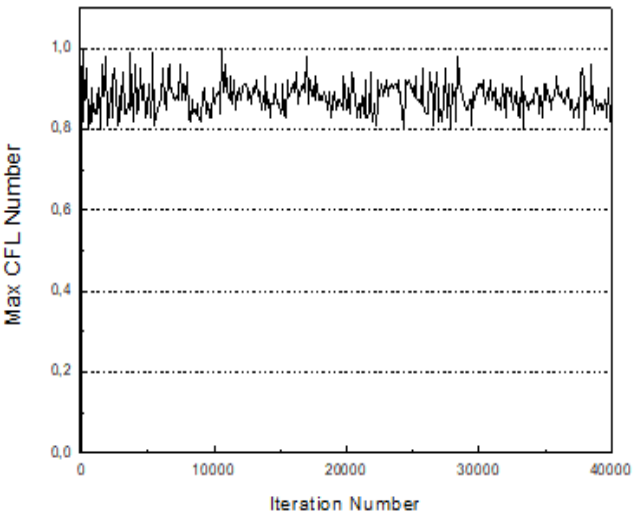

Fig. 2 CFL number for FDS simulation

The Courant–Friedrichs–Lewy (CFL) was used in FDS to assure the stability of the numerical scheme. The CFL condition requires that the CFL number is smaller than 1 and greater than 0.8 (McGrattan et al., 2017b). The CFL condition requires than: $\delta t \max\left(\frac{|u|}{\delta x}, \frac{|v|}{\delta y}, \frac{|w|}{\delta z}\right) < 1$.

The convergence calculation was satisfied with the CFL number varying in the range from 0.80 to 0.99 throughout all simulations. An example of the CFL number is displayed in Fig. 2.

In this study, simulations were conducted on duration to 600 seconds, and the fire heat release rate was treated as an average value.

2.3 Model Validation

The feasibility of FDS for simulating tunnel fires has undergone extensive validation, involving experiments and theoretical models in various previous studies. FDS was used to predict the maximum temperatures beneath the tunnel ceiling, and these predictions were compared with experimental results from Li et al. (2011).

It's worth noting that the experimental data from Li et al. (2011) included reduced-scale tests, which were also compared with data from two full-scale tests. The results indicate a good agreement between the reduced-scale test and the other tests.

The temperature values depend on the heat release rate and the longitudinal velocity of airflow. In this study, we determined the maximum temperature for various heat release rate at different longitudinal airflow. The range of heat release rate values corresponds to those employed in our investigation.

The results, as shown in Table 2, demonstrate that the ceiling temperatures predicted by FDS align well with the experimental data.

Table 2 Comparison table of the Temperature

Q (kW)	3750	5937,5	13437,5	13437,5	16250	18750
U (m/s)	0,190	0,496	0,305	2,673	2,635	2,520
$T_{max,Li}$ **(°C)**	203	349	463	217	271	322
$T_{max,FDS}$ **(°C)**	192	337	449	212	279	329
Error (%)	5,41	3,44	3,02	2,30	2,95	2,17

3. RESULTS AND DISCUSSIONS

In a fire in the tunnel, after the initial radial and transition phases, the behavior of smoke gradually evolves into a one-dimensional propagation. At this stage, the characteristics of smoke layer movement become crucial for safe evacuation and effective smoke control. However, the thermal properties of smoke in tunnel fires require further clarification.

The stratification is influenced primarily by two dominant factors: buoyancy force and inertia force. The fire-induced buoyancy force tends to maintain the stability of the stratified layers of smoke, while the longitudinal inertia forces induced by the airflow mix the layers. Therefore, the degree of stratification induced by the fire depends on the balance between these two competing mechanisms, with a third parameter represented by the inclination of the tunnel, as explored in this study.

3.1 Smoke Layer Stratification State

Figure 3 shows the longitudinal distribution of temperature ratio for Q = 4MW. In the absence of longitudinal velocity air-flow, the recorded values of $(\frac{\Delta T_{cf}}{\Delta T_{avg}})$ exhibit a higher magnitude for positive slopes compared to a slope angle β = 0°. The smoke flow is maintained stratified up to x = 250 m for all cases. Applying a longitudinal velocity, relatively average to the heat release rate, traducing by a good stratification for the smoke layer with β = 0° and the smoke flow destabilizes with increasing the slope.

By applying a longitudinal air flow of 2 m/s for Q = 4MW, the smoke flow is well stratified at β = 3°, as for other cases of β (β = 0 and β = 6°) up to x = 240 m. Note that the values of (ΔTcf / ΔTavg) are between 1.4 and 2, that is to say the flow of the smoke layer is controlled by the longitudinal velocity of fresh air.

By increasing the longitudinal velocity to 3 m / s, the shapes of the curves are sinusoidal and the amplitude for the slopes of 3° and 6° is greater than the slope equal to 0° because the slope increases the inertia force. Adding, the velocity of 3 m/s represent a large inertia force compared to the buoyancy force of a heat release rate of 4 MW. That is, the flow of the smoke layer is totally carried by the inertia force.

For Q = 20 MW, Fig. 4, the flow of smoke layer is stable up to x = 220 m for the slope equal to 0° and it is improved with β = 3° up to x = 240 m, then the flow becomes destabilized from x = 210 m for β = 6°.

By applying a velocity of 1m/s, the flow is well stratified up to x = 230 m then it destabilizes for β = 0° and the flow stratification was decreases for β = 3° then, with increasing of β, it is de-stratified.

The increase of the longitudinal air flow, 2 m / s, favors the stratification of the smoke flow, especially for β = 3°. However, the flow of the smoke layer is controlled by the longitudinal velocity of air for β = 0° and it is destabilized for β = 6° at the last downstream half of the tunnel when Q = 20 MW.

For Q = 20 MW with U = 3 m / s, the flow becomes destabilized and the values of (ΔTcf / ΔTavg) are close across all cases, that is to say the inertia force is greater than that of the buoyancy.

The decrease in smoke temperature along the tunnel ceiling, as described in existing horizontal tunnel literature, needs to be adjusted to account for the tunnel slope factor. The decay in temperature is primarily influenced by heat loss across the boundaries, which is a following of entrainment at the interface of the smoke layer.

In the case of a horizontal tunnel where the gravitational force is perpendicular to the direction of the smoke layer, the entrainment of cold air into the upper hot smoke flow is primarily caused by the shear effect and the mixing at their interface. However, in the case of a sloping tunnel, the entrainment of cold air induced by buoyancy, resulting from the gravitational force, becomes a significant contributing factor. This increased entrainment of cold air into the gas stream leads to a more rapid decrease in gas temperature with distance.

Additionally, in a sloping tunnel, the velocity of the smoke flow is either accelerated or decelerated, as demonstrated in Figs. 3 and 4, particularly when U = 0 m/s, where the buoyancy force has a significant role indicating potential variations in heat transfer characteristics.

Figure 5 shows the longitudinal distribution of temperature ratio with Q = 10MW. For β = 0°, the best cases recorded are those where the smoke flow is guided by the longitudinal velocity of air , i.e. there is a balance between the buoyancy force of the smoke layer and of the inertia force generated by the longitudinal velocity.

Then, with β = 1.5° and Q = 10MW, the best case for the stability of the smoke flwo is at the longitudinal velocity of 2 m/s. On the other, the stratification of flow decreases for 1 and 3 m/s. By increasing β, the best case is for the longitudinal velocity equal to 2 m / s for β = 3°. In the end, β = 6°, the flow is de-stratifed in all cases from x = 210m.

As the downstream from the fire source, when the velocity ranges from approximately 0 to 1 m/s and Q = 10MW, a noticeable temperature difference between the

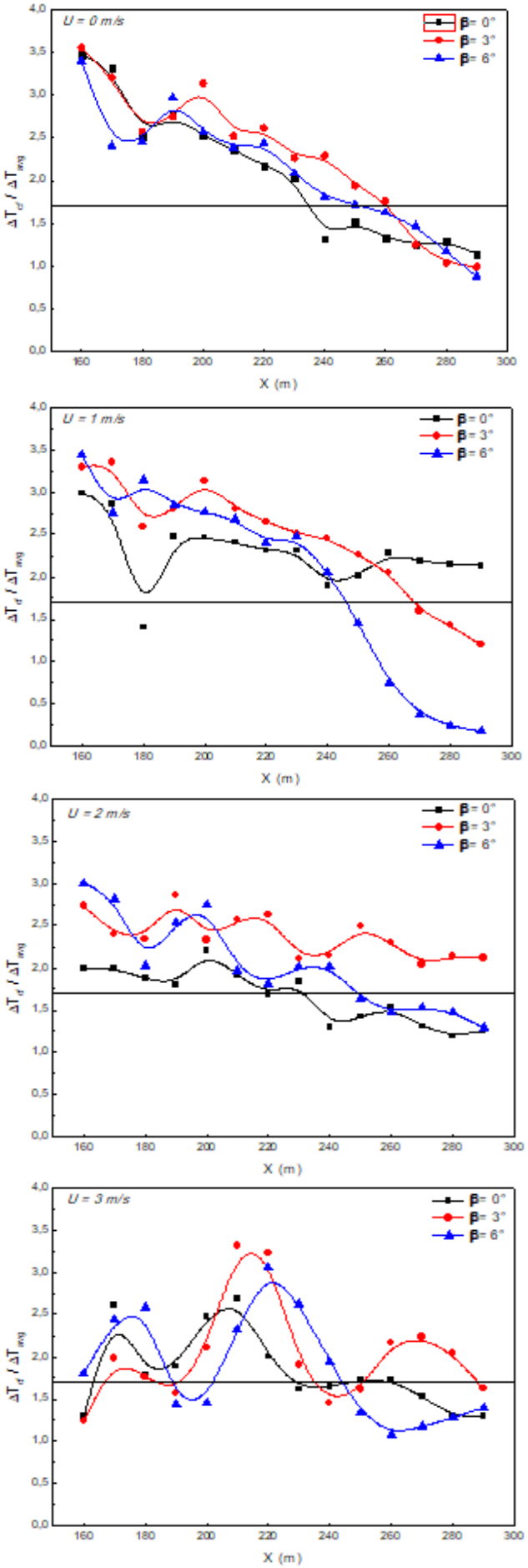

Fig. 3 Temperature ratio distribution at downstream side of tunnel, Q = 4 MW

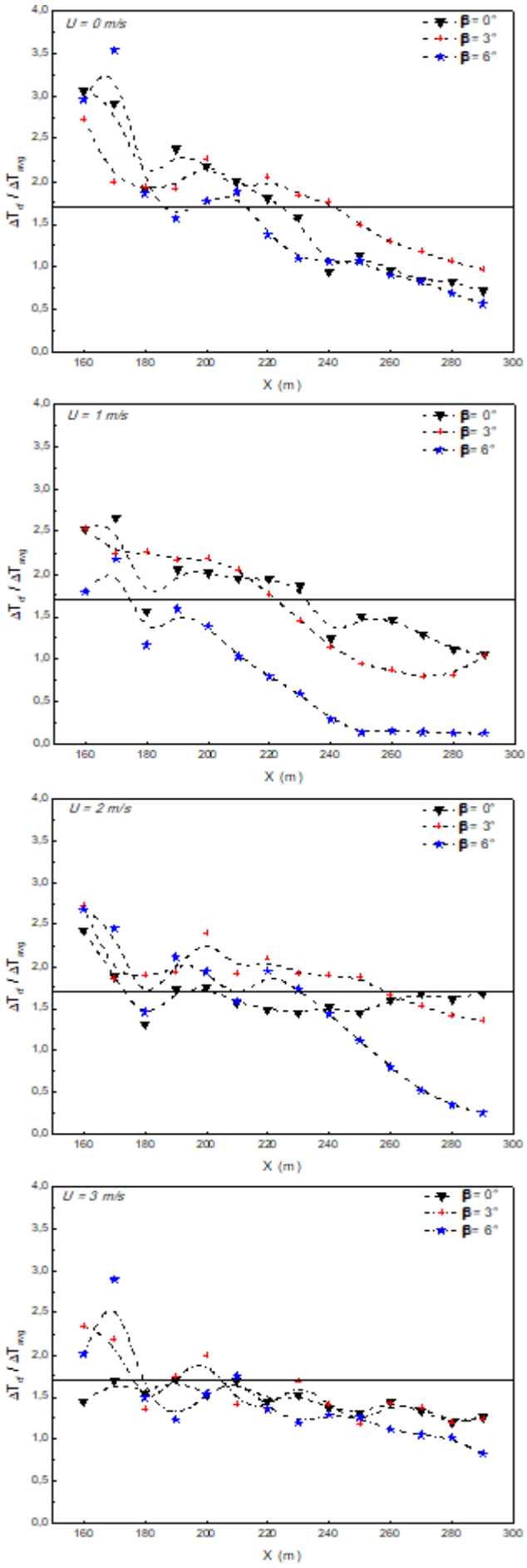

Fig. 4 Temperature ratio distribution at downstream side of tunnel, Q = 20 MW

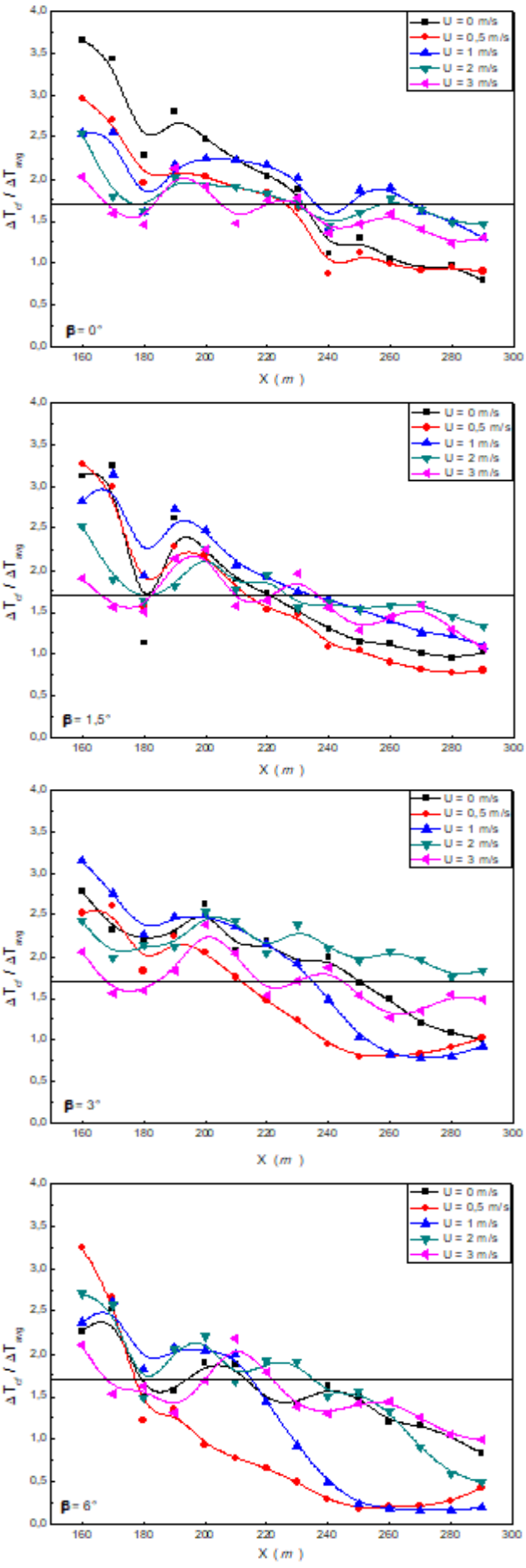

Fig. 5 Temperature ratio distribution at downstream side of tunnel, Q = 10 MW

upper and lower layers becomes evident. Within this tunnel section, the temperature experiences sudden changes, indicating a distinct stratification of smoke. As the longitudinal velocity of the airflow increases, the temperature at the floor level rises, and the temperature difference between the ceiling and the floor decreases.

These findings suggest that smoke stratification decreases. Furthermore, as the velocity continues to increasing, the temperature difference between the ceiling and the floor decreases further.

This trend implies that the vertical temperature distribution becomes more uniform, ultimately leading to the disappearance of smoke stratification.

The influence of the ceiling opening becomes noticeable downstream of the tunnel, approximately the reaching a distance of x = 240 m. At this point, when the velocity ranged from 1 to 2 m/s, the stratification of the smoke weakened and eventually disappeared for velocities of 0 and 0.5 m/s.

The presence of the opening leads to the extraction of a certain quantity of smoke, which subsequently affects the temperature contrast between the ceiling and the floor, resulting in a reduced temperature gradient. However, for velocities exceeding 1 m/s, the flow of the smoke layer is primarily guided by the longitudinal velocity. Additionally, when considering the slope of the tunnel, it's important to note that the opening impact decreases. As the slope of the tunnel continues to increase, the influence of the opening becomes negligible. Furthermore, taking into account the tunnel slope, longitudinal air flow and the heat release rate of the fire, it becomes evident that openings in the ceiling of the tunnel significantly affect the behavior of the smoke layer.

Maintaining the longitudinal velocity within a specific range proves crucial for ensuring a clear stratification of the smoke at a designated distance downstream (as shown in Fig. 5, with β = 0° and U = 1 m/s). When considering the effect of the tunnel's slope, which also facilitates the entrainment of fresh air into the smoke layer, the stratification of the smoke flow can be effectively maintained at a slope of 3° and a longitudinal velocity of 2 m/s across all cases.

3.2 The Model of Smoke Stratification

The buoyancy force and the inertia force, which are the two primary factors governing the stratification of buoyant flow, were correlated using the Froude number. In this paper, the Froude number was calculated based on Eq. (3) with β = 0°.

Figure 6 illustrates the relationship between the Froude number and the temperature ratio, which can be utilized to differentiate between different stratification states. A curve fit of the data resulted in the following equation:

$$\frac{\Delta T_{cf}}{\Delta T_{avg}} = 1{,}12\ Fr^{-1{,}08} \qquad (7)$$

The correlation coefficient for this analysis was calculated to be R^2 = 0.90. When the Froude number (Fr) was less than 1, Eq. (7) closely approximated Eq. (3).

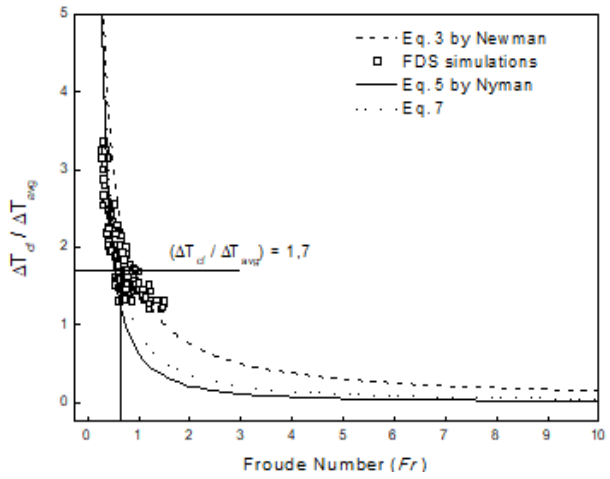

Fig. 6 Relationship of the temperature ratio and Froude number

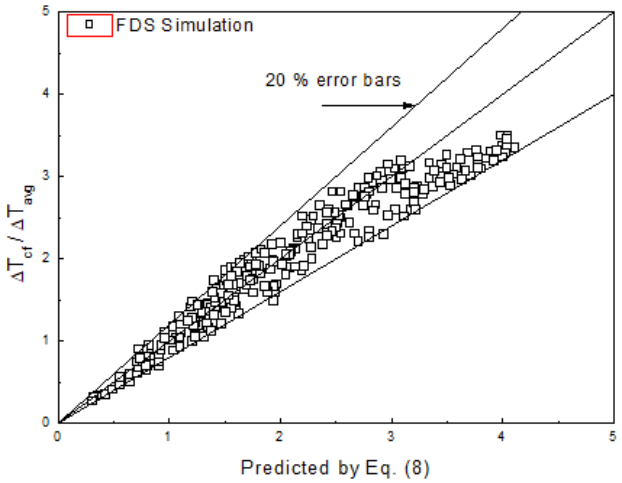

Fig. 7 Relationship between the temperature ratio, Froude number and tunnel slope (Eq.8)

However, both Eq. (7) and Eq. (5) could accurately match to Eq. (3).

Based on Eq. (2), when the ratio $\frac{\Delta T_{cf}}{\Delta T_{avg}} \geq 1.7$ is greater than or equal to 1.7, it indicates clear smoke stratification. Therefore, a Froude number of Fr = 0.63 could be employed as the criterion to determine whether the smoke stratification was evident. This value is close to the one suggested by Nyman (Fr = 0.55). It's important to note that the Froude number used in this study is relatively small compared to the value proposed by Newman (Fr = 0.9).

Overall, *Fr* showed little change, and the Froude number could be used, to represent the stratification criterion in this study, equal to 0.63. The buoyancy of smoke layer is influenced by the tunnel slope and longitudinal air flow. Thus, $\frac{\Delta T_{cf}}{\Delta T_{avg}}$ was related to both *Fr* and β.

Firstly, β as the independent variable, we have a Newman's equation (Eq.3) generate a curve of $\frac{\Delta T_{cf}}{\Delta T_{avg}} = f(Fr)$ as a function of Fr for various β. Subsequently, an adjustment was carried out to establish a correlation between the coefficients as a function of β, the tunnel slope. As a result, presenting the model that provides the relationship between the temperature ratio and the Froude number while accounting for the tunnel slope (β). This model likely offers valuable insights into how these factors interact and influence smoke behavior in tunnel fires. $\frac{\Delta T_{cf}}{\Delta T_{avg}} = f(Fr,\ \beta)$ is as follows :

$$\frac{\Delta T_{cf}}{\Delta T_{avg}} = (1.48 + 0.11\,\beta - 0.026\,\beta^2)Fr^{-1} \qquad (8)$$

It should be emphasized that the model is developed based on the results of the simulation. A correlation coefficient equal to 0.92 was found for Eq. (8).

After having put the model, corresponds to the expression of $\frac{\Delta T_{cf}}{\Delta T_{avg}} = f(Fr,\ \beta)$, Fig. 7 represent the verification of all the cases to simulate.

The predictions made by the modified model (Eq. 8) in this study exhibit a strong agreement with Newman's theory, with the errors less than 2% observed when β approaches 0°. However, for the current model (Eq. 8), the overall error is 20%, as depicted in Fig. 7.

Figure 8 illustrates the relationship between the Froude number and the longitudinal velocity of air-flow for various tunnel slopes with Q = 10MW. As the longitudinal velocity increases, it tends to introduce instability into the flow of the smoke layer. However, when compared to the scenario with β = 0° (a horizontal tunnel), at lower longitudinal velocities in sloped tunnels, both the stability of the flow and the stratification of the smoke layer are enhanced.

When the longitudinal velocity reaches a certain threshold, where the average inertial force equals the buoyancy force, the flow of the smoke layer becomes destabilized. This transition results in complete de-stratification, particularly noticeable for significant tunnel slopes.

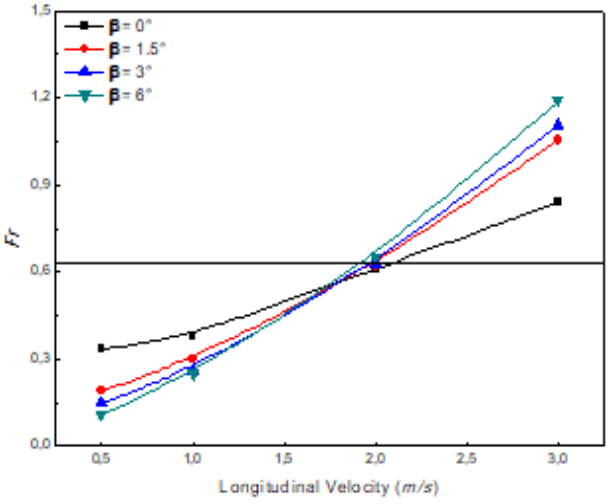

Fig. 8. Froude number function of the longitudinal velocity at *x = 170 m*

As we move downstream in the tunnel, the presence of tunnel slope promotes the de-stratification of the smoke flow layer, particularly when the applied longitudinal velocity exceeds 2 m/s (Fig. 8). This is because the slope accelerates the flow of the smoke layer, causing it to interact with fresh air entering from the tunnel outlet.

It's crucial to strike a balance between the inertia force and the gravitational force, with the slope of the tunnel, to prevent the flow de-stratification.

These findings provide valuable insights for researchers a deeper understanding of the thermal buoyancy phenomena in smoke flow within inclined tunnels. Furthermore, it's essential to continue investigating smoke layer behavior in different tunnel geometries and under varying parameters. This ongoing research will help refine and broaden the applicability of the correlations developed in this study.

4. CONCLUSION

This paper conducted a study on smoke stratification in inclined tunnels, building upon the work of Newman, and considering the combined effects of longitudinal air-flow and tunnel slopes using FDS.

Firstly, the study proposed a correspondence between the temperature ratio and the Froude number, which demonstrated good agreement with the Newman model, especially when the Froude number was less than 1. Furthermore, the dimensionless temperature ratio was estimated using Equation 8, taking into account the Froude number and the tunnel slope.

The research observed that the Froude number increases with higher longitudinal airflow velocity. Along the downstream side, the Froude number displayed a slow increase in the longitudinal direction, especially when the tunnel slope was equal to 0° in comparison to slopes exceeding 1.5°.

In cases where the longitudinal velocity and the tunnel slope have critical values, the smoke in the downstream side of the tunnel became more stable, resulting in a slightly higher temperature ratio.

Increasing both the longitudinal airflow and the tunnel slope serves to disturb the stratification of the smoke layer. This disruption is noteworthy, as it can influence the overall dynamics of smoke movement within the tunnel environment. The intensified longitudinal velocity, coupled with an increased slope, contributes to alterations in the thermal patterns and buoyancy forces, potentially influencing fire safety considerations and evacuation strategies in tunnel scenarios.

In summary, this article provides an insightful study of smoke stratification in inclined tunnels under the influence of longitudinal airflow. It suggests the need for further experiments to investigate how various parameters affect smoke behavior in inclined tunnels.

ACKNOWLEDGEMENTS

The authors thank the Directorate for the Laboratory of Energy, Heat and Mass Transfer (LETTM).

CONFLICT OF INTEREST

The authors declare that they have no known competing financial interests or personal relationships that could have appeared to influence the work reported in this paper.

AUTHORS CONTRIBUTION

B. Kalech: Software, Validation, Investigation, Resources, Data Curation, Text and Figure Formatting, Writing of the Manuscript; **M. Bouterra**: Review and Editing; **A. ElCafsi**: Review and Editing.

REFERENCES

Atkinson, G. T., & Wu, Y. (1996). Smoke control in sloping tunnels. *Fire Safety Journal*, *27*, 335–341. https://doi.org/10.1016/S0379-7112(96)00061-6

Chow, W. K., Gao, Y., Zhao, J. H., Dang, J. F., & Chow, N. C. L. (2016). A study on tilted tunnel fire under natural ventilation. *Fire Safety Journal*, *81*, 44–57. https://doi.org/10.1016/j.firesaf.2016.01.014

Fan, C., Zhang, L., Jiao, S., Yang, Z., Li, M., & Liu, X. (2018). Smoke spread characteristics inside a tunnel with natural ventilation under a strong environmental wind. *Tunnelling and Underground Space Technology*, *82*, 99–110. https://doi.org/10.1016/j.tust.2018.08.004

Guo, Y., Yuan, Z., Yuan, Y., Cao, X., & Zhao, P. (2021). Numerical simulation of smoke stratification in tunnel fires under longitudinal Velocities. *Underground Space*, *6*, 163-172. https://doi.org/10.1016/j.undsp.2019.11.001

Gwon Hyun, K., Seung Ryul, K., & Hong Sun, R. (2010). An experimental study on the effect of slope on the critical velocity in tunnel fires. *Journal of Fire Sciences*, *28*, 27–47. https://doi.org/10.1177/0734904109106547

Haddad, R. K., Zulkifli, R., Maluk, C., & Harun, Z. (2020). Experimental investigation on the influences of different horizontal fire locations on smoke temperature stratification under tunnel ceiling. *Journal of Applied Fluid Mechanics*, *13*(4), 1289-1298.

http://doi.org/10.36884/jafm.13.04.30876

Han, J., Liu, F., Fei Wang, F., Weng, M., & Wang, J. (2020). Study on the smoke movement and downstream temperature distribution in a sloping tunnel with one closed portal. *International Journal of Thermal Sciences*, *149*, 106-165. https://doi.org/10.1016/j.ijthermalsci.2019.106165

Hu, L. H, Fong, N. K., Yang, L. Z., Chow, W. K., Li, Y. Z., & Huo, R. (2007). Modeling fire-induced smoke spread and carbon monoxide transportation in a long channel: fire dynamics simulator comparisons with measured data. *Journal of Hazardous Materials*, *140*, 293–298. https://doi.org/10.1016/j.jhazmat.2006.08.075

Hu, L. H., Chen, L. F., Wu, L., Li, Y. F., Zhang, J. Y., & Meng, N. (2013). An experimental investigation and correlation on buoyant gas temperature below ceiling in a slopping tunnel fire. *Applied Thermal Engineering*, *51*, 246–254 https://doi.org/10.1016/j.applthermaleng.2012.07.043

Huang, Y., Li, Y., Dong, B., Li, J., & Liang, Q. (2018). Numerical investigation on the maximum ceiling temperature and longitudinal decay in a sealing tunnel fire. *Tunnelling and Underground Space Technology*, *72*, 120–130. https://doi.org/10.1016/j.tust.2017.11.021

Ji, J., Gao, Z., Fan, C., & Sun, J. (2013). Large eddy simulation of stack effect on natural smoke exhausting effect in urban road tunnel fires. *International Journal of Heat and Mass Transfer*, *66*, 531-542. https://doi.org/10.1016/j.ijheatmasstransfer.2013.07.057

Ji, J., Guo, F., Gao, Z., & Zhu, J. (2018). Effects of ambient pressure on transport characteristics of thermal-driven smoke flow in a tunnel. *International Journal of Thermal Sciences*, *125*, 210–217. https://doi.org/10.1016/j.ijthermalsci.2017.11.027

Kalech, B., Bouterra, M., & ElCafsi, A. (2020). Numerical analysis of smoke flow under the effect of longitudinal airflow in a tunnel fire. *Fire and Materials*, *44*, 1033–1043. https://doi.org/10.1002/fam.2902

Kalech, B., Bouterra, M., ElCafsi, A., & Belghith, A. (2013). Control of smoke flow in a tunnel. *Journal of Applied Fluid Mechanics*, *6*(1), 49-60 https://doi.org/10.36884/jafm.6.01.19481

Ko, G. H., Kim, H. S. R., & Ryou, S. (2010). An experimental study on the effect of slope on the critical velocity in tunnel fires. *Journal of Fire Sciences*, *28*(1), 27–47. https://doi.org/10.1177/0734904109106547

Li, Y. Z., Lei, B., & Ingason, H. (2011). The maximum temperature of buoyancy-driven smoke flow beneath the ceiling in tunnel fires. *Fire Safety Journal*, *46*, 204–210. https://doi.org/10.1016/j.firesaf.2011.02.002

McGrattan, K., Hostikka, S., McDermott, R., Floyd, J., Weinschenk, C., & Overholt, K. (2017a). Fire dynamics technical reference guide: validation. *NIST Special Publication*, *1018*(3). https://pages.nist.gov/fds-smv/

McGrattan, K., Hostikka, S., McDermott, R., Floyd, J., Weinschenk, C., & Overholt, K. (2017b). Fire Dynamics Simulator: Technical Reference Guide, Volume 1: Mathematical Model. *NIST Special Publication*, *1018*(1). https://pages.nist.gov/fds-smv/

McGrattan, K., Hostikka, S., McDermott, R., Floyd, J.,Weinschenk, C., & Overholt, K. (2017c). fire dynamics simulator: User's guide. *NIST Special Publication*, *1019*. https://pages.nist.gov/fds-smv/

Newman, J. S. (1984). Experimental evaluation of fire-induced stratification. *Combustion and Flame*, *57*, 33–39. https://doi.org/10.1016/0010-2180(84)90135-4

Nyman, H., & Ingason, H. (2012). Temperature stratification in tunnels. *Fire Safety Journal*, *48*, 30–37. https://doi.org/10.1016/j.firesaf.2011.11.002

Savalanpour, H., Farhanieh, B., & Afshin, H. (2021). Effects of false-ceiling oncritical ventilation velocityand maximum gas temperature in tunnel fires. *Journal of Applied Fluid Mechanics*, *14*(2), 473-483. https://doi.org/10.47176/jafm.14.02.31382

Wan, H., Gao, Z., Han, J., Ji, J., Ye, M., & Zhang, Y. (2019). A numerical study on smoke back-layering length and inlet air velocity of fires in an inclined tunnel under natural ventilation with a vertical shaft. International *Journal of Thermal Sciences*, *138*, 293–303. https://doi.org/10.1016/j.ijthermalsci.2019.01.004

Weng, M. C., Lu, X. L., Liu, F., & Du, C. X. (2016). Study on the critical velocity in a sloping tunnel fire under longitudinal ventilation. *Applied Thermal Engineering*, *94*, 422–434. https://doi.org/10.1016/j.applthermaleng.2015.10.059

Yang, D., Hu, L. H., Huo, R., Jiang, Y. Q., Liu, S., & Tang, F. (2010). Experimental study on buoyant flow stratification induced by a fire in a horizontal channel. *Applied Thermal Engineering*, *30*, 872–878. https://doi.org/10.1016/j.applthermaleng.2009.12.019

Yi, L., Xu, Q., Xu, Z., & Wu, D. (2014). An experimental study on critical velocity in sloping tunnel with longitudinal ventilation under fire. *Tunnelling and Underground Space Technology*, *43*, 198–203. https://doi.org/10.1016/j.tust.2014.05.017

Zeng, Z., Xiong, K., Lu, X., Cheng, M., & Liu, W. F. (2018). Study on the smoke stratification length under longitudinal ventilation in tunnel fires. *International Journal of Thermal Sciences*, *132*, 285–295. https://doi.org/10.1016/j.ijthermalsci.2018.05.038